
# Photocatalytic $CO_2$ Reduction by $H_2O$: Insights from Modeling Electronically Relaxed Mechanisms

| | |
|---|---|
| Journal: | *Catalysis Science & Technology* |
| Manuscript ID | CY-ART-10-2018-002046.R2 |
| Article Type: | Paper |
| Date Submitted by the Author: | 19-Jan-2019 |
| Complete List of Authors: | Poudyal, Samiksha; University of Tennessee, Chemical Engineering<br>Laursen, Siris; University of Tennessee, Chemical Engineering |
| | |

Journal Name

ARTICLE TYPE

Cite this: DOI: 10.1039/xxxxxxxxxx

# Photocatalytic $CO_2$ Reduction by $H_2O$: Insights from Modeling Electronically Relaxed Mechanisms

Samiksha Poudyal [a] and Siris Laursen [a,*]

Received Date
Accepted Date

DOI: 10.1039/xxxxxxxxxx

www.rsc.org/journalname

A detailed understanding of the mechanism for photocatalytic reduction of $CO_2$ by $H_2O$ is required to facilitate the development of catalysts that exhibit improved activity, controlled product distributions, and enhanced quantum yield. As the reaction assuredly contains many more reaction intermediates than the well-studied water-splitting reaction, the effect of catalyst surface reactivity may be quite pronounced. The reaction mechanism may also contain electronically relaxed intermediates that are driven through the reaction via non-photoelectrochemical steps. We have investigated the ground-state surface reaction mechanism for $CO_2$ reduction over SiC and GaN using DFT modeling. Results were correlated with experimentally observed catalyst performance at near-ambient and elevated temperatures and in condensed and gas phase $H_2O$ conditions. Positive correlations suggest photocatalyst surface reactivity may play a role in C–O cleavage and stabilizing reaction intermediates to promote $CH_4$ production. Electronic analysis indicated protonic $H^+$ from $H_2O$ dissociation would relax to neutral $H^0$ over SiC – an effect that correlated with elevated performance in $CH_4$ production. Less stable $H^+$ over GaN also correlated with a selectivity preference for $H_2$ production. Overall, results suggest that alternative factors beyond bulk electronic structure dictate photocatalytic activity in this reaction.

## 1 Introduction

Deciphering and controlling heterogeneous photocatalytic synthesis reaction mechanisms is a critical step to enabling the production of fuels and chemicals from sunlight and thermochemically stable molecules like $CO_2$, $H_2$, and $N_2$. Moreover, expanding the understanding of all possible energy sequestration pathways available in photocatalytic environments beyond classical electrochemical reduction and oxidation by excited states may dramatically improve overall efficiency and access to specific products. With respect to efficiency, photocatalysts that utilize lower energy IR radiation or couple with external thermal inputs may dramatically change the landscape of photocatalytic synthesis.

A recent study published by our group focused on understanding the effect of catalyst surface chemistry and autogenously produced elevated temperatures in concentrated solar photocatalytic $CO_2$ reduction has suggested that both photoelectrochemical and vibrationally-driven reaction steps may be used to sequester a larger portion of the total spectrum of sunlight and promote the full reduction of $CO_2$ to hydrocarbons[1]. This effect, albeit sparsely demonstrated, has been encountered in photocatalytic oxidation of ethylene over $TiO_2$ and in $CO_2$ reduction to CO over Si[2,3]. Despite $CH_4$ being the dominant hydrocarbon encountered in clean reaction systems, once the mechanism is understood, catalysts may be designed to promote carbon-carbon coupling for $C_{2+}$ hydrocarbon production.

Efforts focused upon heterogeneous photocatalyst discovery and optimization have dominantly relied upon the bulk electronic properties of materials, properties of the condensed aqueous phase-catalyst interface, and overall thermodynamics of the reactions being performed to predict electron and hydrogen transfer dynamics and catalyst performance in water-splitting and $CO_2$ or $N_2$ reduction[4–9]. This approach has allowed for a good degree of success in the discovery and design of catalysts for water-splitting, but has been significantly less effective directing the design of $CO_2$ and $N_2$ reduction catalysts. The inability to design these catalysts with our current understanding suggests that mechanistic aspects of the photocatalytic $CO_2$ and $N_2$ reduction reaction systems may not be captured well by a purely excited-state and electrochemical-reduction/oxidation treatment of the mechanism where vibrational barriers are assumed to be surmountable at or near room temperature. If more significant vibrational barriers were present in the mechanism, elevated reaction temperatures would be required to achieve activity. However, elevated temperatures are ostensibly considered detrimental to catalytic activity because of $e^-/h^+$ recombination[2,10]. This

[a] Department of Chemical and Bimolecular Engineering, University of Tennessee, Knoxville, Tennessee 37909, United States. Fax: (865) 974-7076; Tel: (865) 974-5786; E-mail: slaursen@utk.edu

† Electronic Supplementary Information (ESI) available: [details of any supplementary information available should be included here]. See DOI: 10.1039/b000000x/

view has been brought into question by recent studies by ourselves and others that have illustrated that elevated temperatures (up to 350°C) achieved through ancillary electrical or autogenous heating by infrared absorption can be quite beneficial for achieving complete reduction of $CO_2$ [1–3,11]. Kinetic isotope effect studies using $D_2O$ have also suggested that there are vibrational barriers within a photocatalytic reaction mechanism that are in fact kinetically important [12–14]. These studies suggest that there may be a simple combination of photoelectrochemical and thermochemical reaction steps in the mechanism or a more complex phenomenon where electronically excited intermediates are not sufficiently destabilized and a non-innocent vibrational barrier still is present in their consumption.

Recent efforts by others in modelling photocatalytic surface reactions over $TiO_2$ have employed either an induced Fermi level shift by loading the model slab with additional atomic H or with electrochemical approaches developed in the field of electrocatalysis [8,15,16]. Within the context of $CO_2$ reduction by $H_2O$ over stoichiometric $TiO_2$, Ji and co-workers utilized atomic-H-laden $TiO_2$ slabs as model surfaces for the hydrogenation of $CO_2$ to $CH_4$ [15,16]. This approach utilizes the inherent effective electronegativity of $TiO_2$ to pull electrons from adsorbed atomic H artificially populating states that would otherwise be empty. Significant adsorbate-adsorbate repulsion and a highly reduced $TiO_2$ electronic structure produced reaction mechanism energetics that suggested $TiO_2$ would be able to reduce $CO_2$ to $CH_4$ without the need for a co-catalyst. In comparing with organic-contamination-free studies of the activity of $TiO_2$, this approach appears to be unrealistic, i.e., properly designed and cleaned reactors with clean $TiO_2$ show no activity in the photocatalytic reduction of $CO_2$ by $H_2O$ only [1,17,18].

Another approach using the computational hydrogen electrode framework for studying the photocatalytic reduction of $N_2$ over Fe-doped, oxygen-vacancy rich, and stoichiometric Rutile $TiO_2$ (110) model surfaces predicted that only the more reactive oxygen-vacancy rich $TiO_2$ surface exhibited surface reaction and redox energetics that would suggest a potential for activity in the reaction [19]. Cleavage of the N–N bond was found to still be kinetically limiting and likely not possible near ambient temperature. Several assumptions in this approach may affect the applicability of the use of the computational hydrogen electrode. Specifically, that the reactions are performed in the gas phase in the absence of an electrolyte. This draws into question the energetics associated with the source of $H^+$. Most notably the effect of the surface reactivity of the catalyst where $H^+$ is bound. As few reliable experimental studies exist for this reaction system [20], it is still unclear whether this modeling approach is valid or not.

A follow-up study by the same group has suggested that the view of the mechanism has changed, and that carbon contaminants present on the catalyst surface serve as critical co-catalyst radical species that promote activation of $N_2$ [21]. This suggestion is more in line with the understanding that organic-contamination-free $TiO_2$ is completely inactive in photocatalytic reactions that require H-transfer for hydrogenation or $H_2$ evolution when a metal co-catalyst is absent [1,17,18,22].

It is important to note that approximations are still very much necessary in efforts to model photocatalytic systems at this point since capturing the dynamics of excited states with respect to driving surface reactions is very computationally expensive or impossible at this time. A very limited selection of studies have begun to treat these systems more exactly, but have been limited to $TiO_2$ and were focused only on the hydrogenation of $CO_2$ without considering C–O bond cleavage pathways due to computational cost [23].

Our approach was to utilize a ground-state Density-Functional Theory (DFT) modeling approach to shed light upon observed catalytic performance of SiC and GaN photocatalysts in $CO_2$ reduction by $H_2O$. Through comparisons with experimental results, the validity of the approach could be determined. SiC and GaN were chosen because they present appropriate band gaps, band edge alignments, and a range of bulk material and surface chemical properties. Appropriate band edge alignments avoided the complication of including co-catalysts in the analysis. The primary mechanistic question was how catalyst surface reactivity and intermediate stability correlated with observed catalytic performance, but the investigation ultimately also suggested the potential for a new H-transfer mechanism over semiconductors comprised of less electronegative p-block elements, e.g., carbon vs nitrogen. Because we are modeling a ground-state reaction mechanism, it is expected that appropriately endothermic overall and stepwise reaction thermodynamics will be encountered. No extra charge or excited states were included in the calculations. The model systems or computational approaches were not modified to artificially produce exothermic reaction energetics, as in previous modeling efforts by others [15,16]. Capturing these energetics will help to shed light upon the nature and magnitude of energy inputs needed to drive the reaction forward.

The validity of the insights gained in the study was determined by comparing with our recently published experimental results that show photocatalytic $CO_2$ reduction is dramatically enhanced over specific catalysts at elevated autogenous temperatures (up to 350°C) under concentrated solar photoreaction (CSPR) conditions and with the published results of others at and above ambient temperature conditions. Comparisons were made only with studies that could be verified to the best of our ability to be organic-contamination free. As organic contamination is rife in the field, extreme scrutiny of all published work was necessary in this regard. If the study did not employ appropriate control tests, isotope tracking, or showed activity for pure $TiO_2$ in the reaction, it was deemed unreliable and not used for comparison.

As experimental results are available across a wide range of temperatures (25°C to 350°C), vibrational kinetic barriers were calculated throughout the mechanisms. The presence of this data does not suggest that these barriers will control the kinetics of the reaction when driven photoelectrochemically, but can shed light upon any effects that are associated with reaction steps that present vibrational barriers low enough to be kinetically accessible at the temperatures considered.

The possibility of vibrational excitation through applied thermal energy or non-radiative relaxation of hot electrons are also considered as potential energy sources since concentrated solar photocatalytic activity data at a temperature of 350°C is now available for comparison [1]. The latter phenomenon has the po-

 

tential to drive non-redox reaction steps that would otherwise be insurmountable through direct heating and has been evoked in plasmon-assisted photocatalytic reactions recently[24]. In electron-mediated desorption studies of atomic H over Ru(111), a femtosecond laser excitation (800 nm, 60 J/m$^2$ fluence) was utilized to produce electronic temperatures of nearly 3000K that promoted $H_2$ evolution and exhibited a kinetic isotope effect using $D_2$[12]. Electron-mediated associative desorption over metals and oxides has also been demonstrated[25–29]. As atomic H on SiC relaxes to neutral charge, this mechanism may be active in driving reactions on the SiC surface.

## 2 Computational Method

Density functional theory (DFT) calculations were performed utilizing Vienna *ab initio* simulation package (VASP 5.3.3) and resources from Extreme Science and Engineering Discovery Environment (XSEDE)[30]. The generalized gradient approximation (GGA) exchange-correlation functional PBE-sol was employed, as it has been reported to accurately capture the electronic structure and bonding within semiconductor solids[31,32]. Specifically, PBE-sol has been shown to capture the band gap of a large suite of semiconductors within 1-2% of experimentally measured values[31,33]. An ultra-soft pseudopotential was utilized to model the hydrogens. Positive and negative reaction energetics quoted throughout the manuscript indicate endothermic and exothermic energies, respectively. Periodic boundary conditions were utilized to model infinite slabs of materials to negate edge effects and to ensure fully developed bulk-like electronic structures were present. Forces within the calculations were relaxed to a value of less than 0.1 eV/Å. A planewave cutoff energy of 400 eV was utilized. The effect of thickness of slabs was investigated, which contributed only 0.02 eV to the reaction mechanism energetics. Surface unit cells of 2x2 and 3x3 were utilized for GaN and SiC, respectively with at least 4 stoichiometric layers. Periodic slabs were separated by a 15Å vacuum gap in the z-direction. For the reaction energetics calculations, two topmost stoichiometric layers of the slab along with the adsorbates were allowed to relax while the rest of the atoms in the slab were fixed. K-point meshes of 2x2x1 and 4x4x1 were utilized for the 3x3 and 2x2 slabs, respectively to sample the Brillouin zone. Adsorption energies as a function of k-point sampling were checked and the selected meshes provided sufficient accuracy at a reasonable computational cost. To ensure that electronic relaxation of adsorbed atomic H did not affect reaction energetics, each H atom was balanced with an OH* group. Activation barriers for reaction steps were calculated using climbing nudged elastic band (cNEB) or DIMER methods[34,35]. The models were optimized until forces were less than 0.1 eV/Å. The INCAR files for the NEB and DIMER methods are provided in the ESI pg. S15-S17.

The oxidation state of the surface-bound H atoms were calculated using Bader charge analysis[36,37]. The surface termination of SiC and GaN were determined using an *ab initio* thermodynamics approach[38–41], which is described in detail in the ESI pg. S1. The GaN surface facet of (0001) was utilized in our study since this surface facet has been determined to be of lowest surface energy via both computational and experimental surface science studies[42–44]. The most favorable surface facet for SiC was determined manually by comparing the surface energies of several C-terminated candidate facets. The C-terminated beta-SiC surface of ($\tilde{1}\tilde{1}\tilde{1}$) surface was found to be lowest in energy and employed in our study. Due to asymmetry in the crystal in the z-direction, the bottom of the slab was Si terminated. To reduce the effects of surface states produced at the bottom of the slab, all dangling bonds were saturated by OH groups.

## 3 Results

### 3.1 Reaction Mechanism Determination

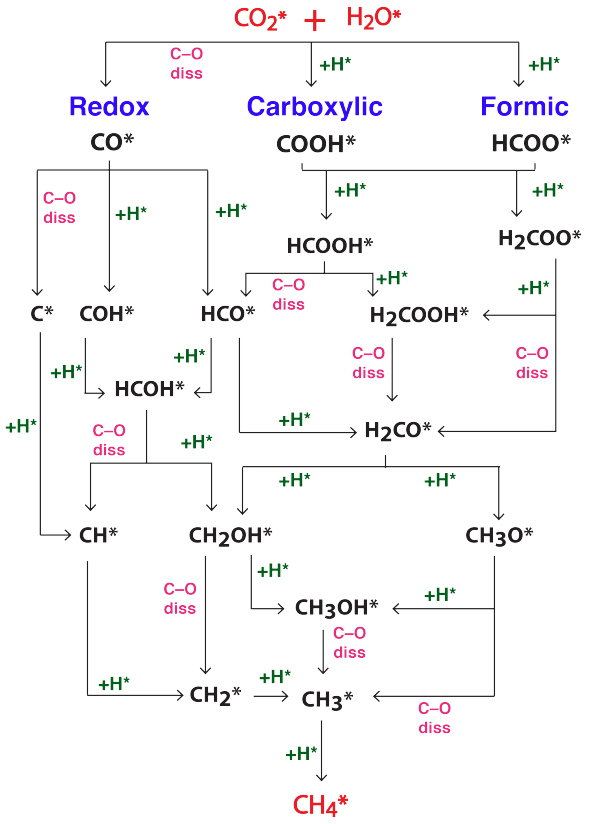


**Figure 1:** Surface reaction pathways considered in $CO_2$ photocatalytic reduction with $H_2O$ to produce $CH_4$. The reduction mechanism initiates via three main pathways: (i) redox, (ii) carboxylic, and (iii) formic routes. All possible reaction pathways via multiple hydrogenation of $CO_2$ were calculated to isolate the most favorable reaction mechanism towards $CH_4$ production.

The most energetically favorable reaction pathways over SiC and GaN were determined via an exhaustive search. All possible reaction sites and reaction network pathways that were chemically reasonable were investigated. Thermodynamics and vibrational kinetic barriers were calculated for all pathways. The least energetically demanding pathways were selected as "most promising", but because the energy available for the reaction system is not well understood, other pathways close in energy may also be active. The reaction network in Figure 1 illustrates all possible reaction pathways that were investigated in our study. It is noted that reaction pathways where C–O bonds are broken and reformed

multiple times were not considered as reasonable in our search. We assume that once a C–O bond has broken, it does not reform favorably along the path to the selective product $CH_4$.

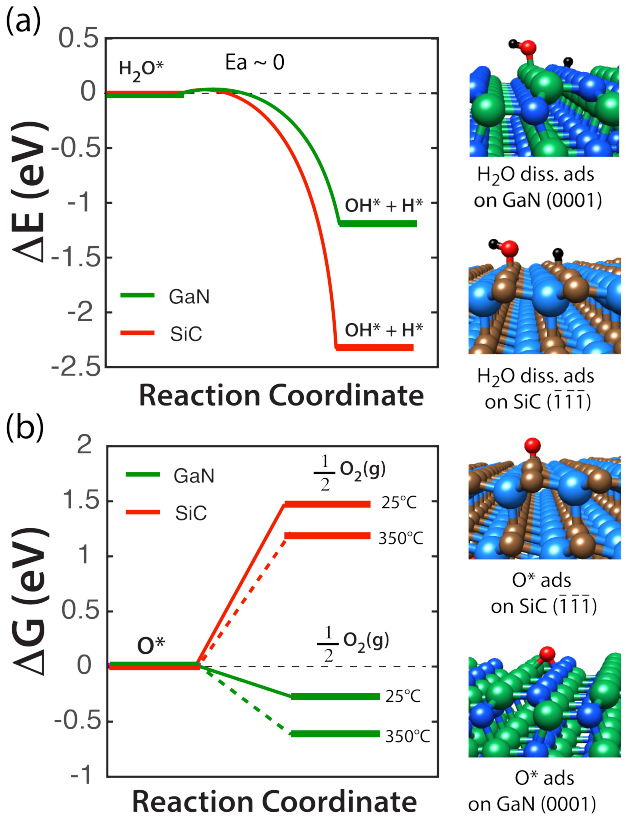


**Figure 2:** (a) $H_2O$ dissociation energetics over SiC and GaN. Significant thermodynamic driving forces towards $H_2O$ dissociation with low kinetic barriers ($E_a \sim 0$ eV) were encountered over both materials and (b) Gibbs free energy of 1/2 $O_2$ molecule evolution over SiC and GaN at 25°C and 350°C. Energetics suggest that $O_2$ evolution may be readily promoted over GaN, while it might be difficult over SiC due to high oxophilicity.

The initiation of $CO_2$ reduction is possible via three pathways: i)redox (direct cleavage of first C–O bond to form CO*), ii) formic (hydrogenation to form HCOO*), or iii) carboxylic (hydrogenation to form COOH*). The redox pathway via electrochemically-promoted direct dissociation of $CO_2$ has been suggested as energetically unfavorable[45,46]; however, may be possible via thermochemical routes over catalysts that exhibit higher surface reactivity towards carbon and oxygen. Over surfaces that present lower surface reactivity, hydrogenation to destabilize C–O bonds before cleavage may be necessary. The formic (HCOO*) and carboxylic (COOH*) routes initiate this destabilization of $CO_2$ through hydrogenation and differ solely with respect to where the initial hydrogenation takes place. Beyond the first hydrogenation, further hydrogenation may be necessary to destabilize C–O bonds enough to be cleaved. Therefore, all possible intermediates of the form $H_xCO_yH_z$ were investigated. After the first C–O cleavage, similar reaction pathway turning points are present as well as varying degrees of C and O hydrogenation needed before 2nd C–O cleavage is accessible.

Water dissociation was studied first since the reaction cannot proceed without the hydrogen it supplies. Because of the stability of $H_2O$, its dissociation is often suggested as a kinetically limiting step in photocatalytic water splitting and $CO_2$ reduction over oxide and nitride-based catalysts[47]. Our results indicate that both SiC and GaN are able to dissociate $H_2O$ with significant thermodynamic driving forces (–2.26 eV and –1.08 eV, respectively) and with nearly zero kinetic barriers (+0.05 and +0.02 eV, respectively). These results agree well with existing surface science experimental and computational studies focused on the surface chemistry of GaN and SiC[42–44,48–52]. Facile $H_2O$ dissociation encountered over both SiC and GaN suggests that this step is not kinetically limiting even at ambient conditions. Likewise, this surface chemical feature suggests that high surface coverages of H* and OH* may be present under reaction conditions and that the fragments may act as catalytic poisons if they are not removed through hydrogenation or $H_2$ and $O_2$ evolution steps. With high H* and OH* coverage, the concentration of carbonaceous species on the catalyst surface, including $CO_2$, may be significantly limited leading to a reduction in overall activity or shifts in product selectivity that favor $H_2$ production. This phenomena could be detrimental at low temperatures in condensed aqueous phase reaction conditions where the chemical potentials of $CO_2$ and $H_2O$ are at a great imbalance. Conversely, it may be absent when utilizing elevated temperatures and gas phase reaction environments were $CO_2$ and $H_2O$ chemical potential can be readily tuned.

In determining the dominant mechanisms across a wide range of reaction conditions, e.g., ambient vs. 350°C, condensed liquid vs. gas phase, AM1.5 vs. 100's of suns, it is assured that several reaction pathways may be active and condition dependent. Potentially unrealized H-transfer mechanisms over non-oxide/nitride catalysts may also enable significantly elevated electronic temperatures that allow higher energy pathways to be catalytically important. The lowest energy pathways will be discussed as well as mechanisms that are more energetically demanding.

Considering the pathways up to the first C–O bond cleavage step, the redox and carboxylic pathways were found to be most favorable over SiC and GaN, respectively. The higher surface reactivity of SiC readily drove the direct dissociation of $CO_2$ to CO* and O* ($\Delta E$ = –0.50 eV, $E_a$ = 0.28 eV). Comparatively, hydrogenations of $CO_2$ over SiC in the carboxylic and formic routes were significantly more energetically demanding ($\Delta E$ = +1.80 and +1.65 eV, and $E_a$ = 2.68 and 2.88 eV, respectively). Over GaN, two hydrogenation events to produce COOH* and HCOOH* were necessary to enable cleavage of the 1$^{st}$ C–O bond due to the lower surface reactivity of material. Moderately endothermic 1$^{st}$ C–O cleavage via dissociation of HCOOH* intermediate was encountered ($\Delta E$ = +0.30 eV and $E_a$ = 1.10 eV). On the contrary, direct $CO_2$ dissociation over GaN was found to be highly energetically unfavorable ($\Delta E$ = +3.78 eV, $E_a$ not calculated). By comparison, hydrogenation steps that lead to 1$^{st}$ C–O cleavage over GaN were significantly more energetically demanding ($\Delta E$ = +0.89 eV and +1.52 eV, $E_a$ = 1.56 and 2.21 eV, respectively) than over SiC. Results suggest that CO* may be produced over SiC readily and is not a rate-determining step. While over GaN, hydrogenation must be achieved twice before the 1st C–O cleavage is accessible. These energetics may directly affect the CO production over the

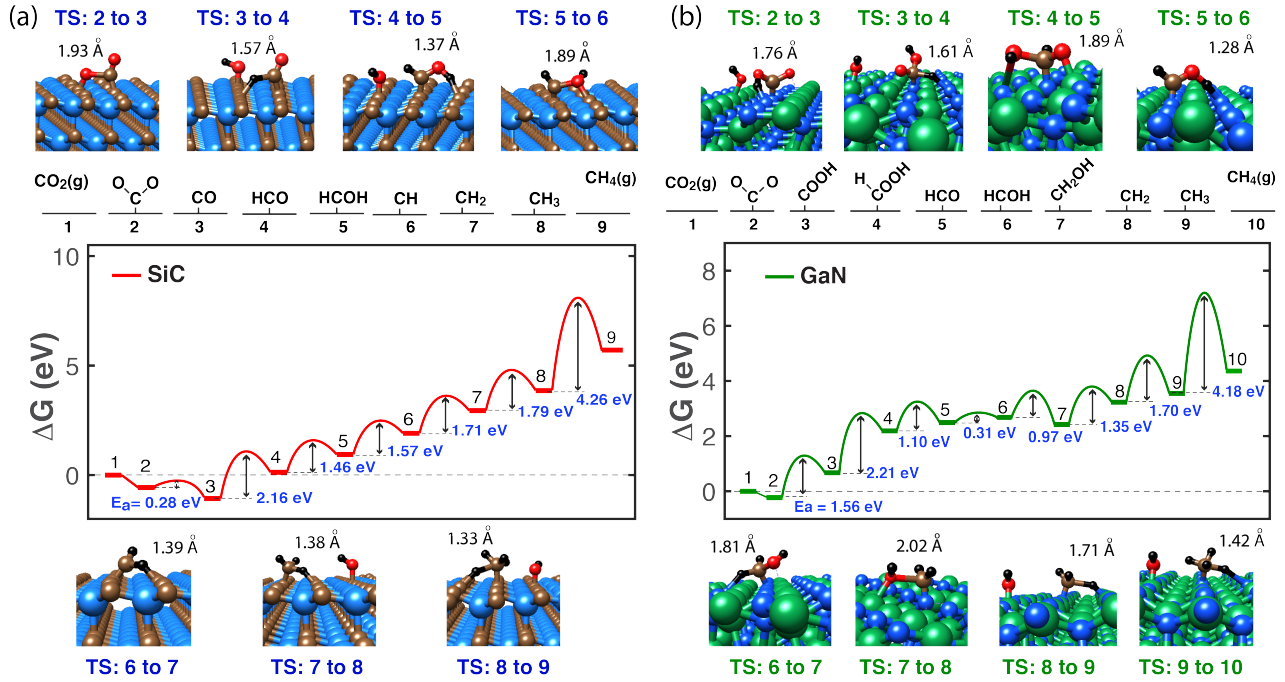


**Figure 3:** Most favorable surface reaction mechanisms isolated for $CO_2$ reduction over (a) SiC and (b) GaN towards $CH_4$ production via ab initio thermodynamics approach (T = 350 °C and ambient pressure). Redox and carboxylic routes were isolated as most favorable pathways for the initiation of $CO_2$ reduction over SiC and GaN, respectively. The model figures illustrate the transition states isolated in between each reaction step. Bond lengths of the transition states are indicated above the model figures.

two catalysts and their general ability to utilize $CO_2$.

In the pathways that promote $2^{nd}$ C–O cleavage, hydrogenation of intermediates was necessary over both SiC and GaN, albeit, to a lesser degree over the more reactive SiC. The formic-like route via a HCO* intermediate was found dominant over SiC (ΔE= +1.19 eV and $E_a$ = 2.16 eV). By comparison, the redox route via the C* intermediate (ΔE = +2.01 eV and $E_a$ = 3.1 eV) and the carboxylic route via the COH* intermediate (ΔE = +3.10 eV and $E_a$ = 4.67 eV) were found to be significantly less favorable. A second hydrogenation of HCO* to HCOH* (endothermic by ΔE = +0.81 eV and $E_a$ = 1.46 eV) was necessary to further destabilize the C–O bond before its dissociation over SiC. The C–O cleavage of HCOH* was found to be moderately endothermic (endothermic by +0.97 eV and $E_a$ = 1.57 eV).

Over the less reactive GaN, two hydrogenation steps prior to second C–O cleavage were found to be necessary. Hydrogenation of HCO* to HCOH* (endothermic by ΔE = +0.18 eV, $E_a$ = 0.31 eV) and then to $CH_2OH$* (exothermic by ΔE = -0.26 eV, $E_a$ = 0.97 eV) were required to destabilize the remaining C–O bond sufficiently. Following hydrogenation, moderate endothermicity towards second C–O cleavage (endothermic by ΔE= +0.81 eV, $E_a$ = 1.35 eV) was encountered. The alternate pathway of C–O dissociation in the HCO* intermediate was significantly less favorable (ΔE = +3.53 eV, $E_a$ not calculated).

Hydrogenation of the $CH_x$ fragments to $CH_3$ over either catalyst was moderately endothermic (SiC: ΔE = +0.93 to +1.03 eV and $E_a$ = 1.71 to 1.79 eV; GaN: ΔE = +0.81 eV and $E_a$ = 1.70 eV). The final hydrogenation of $CH_3$* to $CH_4$ was found to be most energetically demanding over both catalysts and was a likely candidate for the rate-determining step (GaN: ΔE = +1.99 eV and $E_a$ = 4.18 eV, SiC: ΔE = +2.77 and $E_a$ = 4.26 eV). Despite the energetics of this step, experimental observations by our group and others indicate that the reaction proceeds to $CH_4$ production [1,53]. However, there are significant differences in overall catalytic activity and $CH_4$ vs. $H_2$ selectivity between SiC and GaN [1]. These results also agree well with results from in situ experimental investigations that tracked intermediates via DRIFTS and EPR spectroscopies [8,54,55]. Most notably, $CH_3$* radicals were the only species identified besides H* radicals, which is expected if the removal of the species is significantly kinetically limited [8,54]. The stability and rigid tetrahedral geometry of this species are likely causes for its difficult removal.

The positive effects of elevated surface reactivity of the photocatalyst in driving C–O cleavage steps may also have a detrimental effect on $CH_4$ or $O_2$ evolution. In the context of $O_2$ evolution, general surface oxophilicity must be directly investigated. The oxophilicity of the semiconductor is a strong function of the electronegativity of the the non-metal element. The Gibbs free energy of $O_2$ evolution (per oxygen atom) was calculated as –0.61 eV/O and –0.27 eV/O over GaN (calculated at 350°C and 25° under ambient pressure), respectively and ambient pressure reaction conditions). Over SiC, $O_2$ evolution (per oxygen atom) was less favorable ( +1.17 eV/O and +1.50 eV/O, at 350°C, same conditions). Results suggest that $O_2$ evolution would be readily promoted over GaN considering its valence band alignment and low reactivity towards atomic oxygen [56,57]. Despite an appropriate valence band alignment for $O_2$ evolution in the case of SiC, $O_2$ evolution may be difficult due to the high oxophilicity of SiC. Due

to the electronegativity of O, $O_2$ evolution may not be as easily promoted through vibrational excitation. These results agree well with the understanding that partially oxidized layers form readily on pristine SiC surface even under ambient conditions [1,58,59]; however, full oxidation to $SiO_2$ even under highly energetic photocatalytic reaction conditions at 350°C [1]. Oxides/nitrides are known to be relatively good oxygen evolution catalysts [60,61].

### 3.2 Oxidation State of Surface-bound Atomic H

**Table 1** Calculated Bader charge analysis of atomic H adsorbed on SiC and GaN surfaces. Two distinct types of surface bound atomic H were encountered – protonic over GaN and neutral over SiC. The charges are reasonable considering the electronegativity of the constituent atoms and the electronegativity of H atom (2.2).

| Catalyst | $\Delta E_{H*}$(eV) | Charge on H ($e^-$) | Electronegativity |
|---|---|---|---|
| SiC | -2.50 | +0.04 | Si (1.9), C (2.5) |
| GaN | -0.66 | +1.0 | Ga (1.8), N (3.0) |

The oxidation state of hydrogen may also be an interesting tunable parameter if non-oxide/nitrides are used as photocatalysts. The hydrogen from $H_2O$ is often assumed to be protonic and significantly affected by the gas-liquid interface, yet as the field moves to using semiconductors comprised of p-block elements that are less electronegative than O and N, atomic $H^+$ may electronically relax to neutral $H^0$. This effect is already evident when $H_2O$ dissociates over less electronegative transition metals [50,62–64]. It is also likely present in any photocatalyst where $H^+$ is reduced at a metal co-catalyst surface [62,64]. Anionic H may also be accessed over Si, as known from hydrogen sensor work [50,65]. The presence of photocatalytically active neutral atomic H may indicate new vibrational H-transfer mechanisms are possible. This phenomenon may play a role in determining the hydrogenation vs. $H_2$ evolution selectivity. Our elevated temperature photocatalytic $CO_2$ reduction results already suggest that these mechanisms exist and are not wholly thermally driven, i.e., photon absorption still drives the reaction [1]. Charge analysis of atomic H adsorbed at the C and N of SiC and GaN indicated that $H^+$ does indeed relax to $H^0$ over SiC and not over GaN (see Table 1). These results are consistent with the electronegativity of Si, C, Ga, and N and agree with established experimental surface science understanding [62,63,66,67]. How this feature of the reaction system affects catalyst activity or selectivity has not yet been directly studied, but comparisons with literature indicate it significantly affects selectivity.

### 3.3 Stability of Reaction Intermediates and Probe Adsorbates

The factors of the photocatalytic system that affect selectivity in $CO_2$ reduction by $H_2O$ are still not well-established, but considering the high energy environment, it is reasonable to suggest that more stabilized intermediates may improve hydrocarbon production by limiting the energetic driving force for reverse reactions and entropic driving forces that favor small molecule production (CO and $H_2$). In an attempt to develop a generally applicable descriptor that would track directly with catalytic activity and product distribution in photocatalytic synthesis reactions, we investigated the general reactivity of SiC and GaN towards both

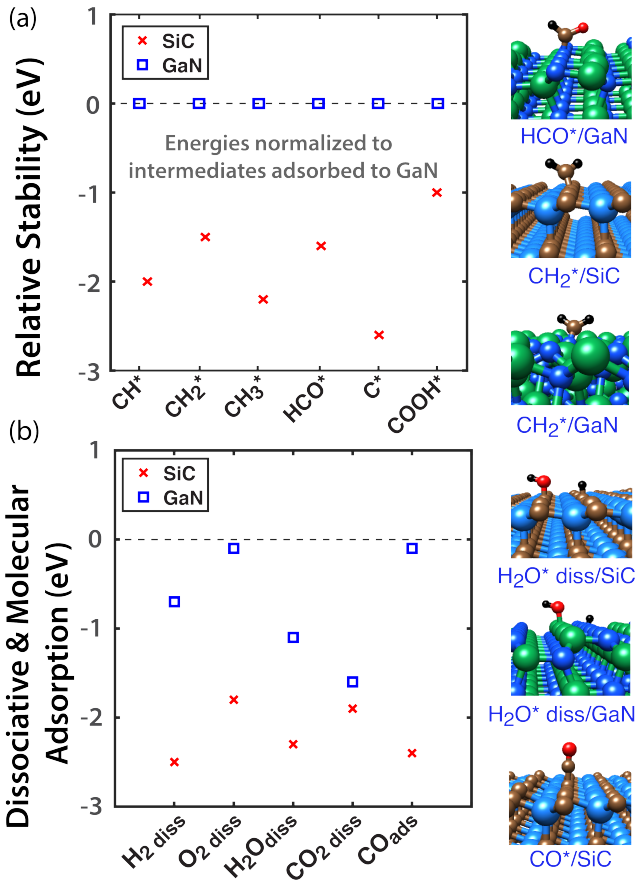


**Figure 4:** (a) Relative stability of key reaction intermediates encountered in the $CO_2$ reduction pathway towards $CH_4$ formation over SiC and GaN. Energetics suggest that SiC exhibits a reactive surface that binds all key reaction intermediates more strongly in comparison to GaN by at least 0.9 eV. (b) Dissociative and molecular adsorption energy (eV) of probe molecules. Similar differences is observed over the two materials in this case.

relevant probe molecules via molecular and dissociative adsorption ($H_2$, $O_2$, $CO_2$, $H_2O$, and CO) and the raw stability of some key intermediates/descriptors that may be catalytically important (CH*, $CH_2$*, $CH_3$*, HCO*, C*, and COOH*). These key intermediates were chosen as probes to understand how catalyst surface reactivity may contribute to promoting C–O bond cleavage and how their stability may track with observed thermal effects in dictating catalytic activity and product selectivity. Stability of the intermediates was used to suggest where vibrational barriers may be appreciable and how catalyst surface reactivity induces this effect. The greater reactivity of SiC is again readily apparent in comparison to GaN with both probe adsorbate and intermediates binding more strongly by at least 0.9 eV (see Figure 4). The elevated reactivity of SiC is clearly responsible for driving

the 1st C–O bond cleavage of $CO_2$. Whereas, several hydrogenations of $CO_2$ over GaN was necessary before C–O bond cleavage could occur. The stabilization of the intermediates may also promote coupling reactions on the surface like hydrogenation or C–C bond formation by combating the entropic driving force for small molecule production. Comparisons with observed experimental activity and the effect of reaction conditions presented later further clarify these connections.

## 4 Discussion

Results thus far suggest that the surface chemistry of photocatalysts may play a significant role in determining surface reaction mechanisms, catalytic activity, and product distributions in a similar fashion as electrocatalysis. Additionally, charge analysis of atomic H on SiC and GaN suggests that non-electrochemical H-transfer mechanisms may be active over SiC where atomic H is of neutral charge. The ground-state neutral atomic H encountered over SiC suggests that H-transfer may be driven by electron-phonon coupling that results in significant vibrational excitation and destabilization of the adsorbate. We now compare to other computational and experimental surface science and catalytic performance studies to ascertain whether these studies can shed light upon the behavior of real photocatalytic systems. Again, we compare only to catalytic performance studies that could be verified to be free of organic contamination through thorough control or isotope tracking studies. Because contamination effects in published literature are abundant, a fairly limited selection of studies could serve as a comparison.

### 4.1 Correlation of Computationally-Derived Mechanisms and Established Surface Science Understanding

Focusing first on the surface chemistry of GaN, $H_2O$ dissociation over single crystal GaN(0001) has been shown to be appreciable and kinetically accessible even at low temperatures via UPS and AP-XPS surface science studies[42,48] as well as in other computational studies[44,49], which agree well with our results. Atomic H adsorption has been reported as moderate with thermal $H_2$ evolution possible at temperatures above ∼250°C in UHV HREELS and TPD studies over single crystal GaN(0001)[68].

The elevated reactivity of GaN towards oxygen has been demonstrated by its oxidation under $O_2$ at ambient conditions. The element mobility in GaN also allowed for a moderately thick native (full) oxide overlayer to form (0.5-2nm thick)[69]. The propensity for surface oxidation is also demonstrated by the need for its removal in electronics applications through acid or base etching of GaN[70,71]. However, even after these treatments, a significant amount of oxygen still persists (∼30% of O per N detected in 1-5 nm of surface of GaN via Auger electron spectroscopy)[70]. GaN has also been shown to be more reactive than $TiO_2$ in the study of ethanol dissociation[72]. This elevated reactivity and ease of oxidation may be detrimental under all reaction conditions, yet post-reaction characterization of photocatalysts is sparsely performed. Our post-reaction characterization of GaN after CSPR conditions for 12 hrs indicated half the material was converted to Ga oxide[1]. The photon absorption environment appears to not limit this effect significantly. Although, the bulk electronic structure of GaN (alignment of VBM with $O_2$ oxidation potential) predicts $O_2$ evolution should be possible, the effect of elevated surface reactivity clearly promotes surface oxidation instead. This illustrates how the classical approach of using bulk electronic properties may fail to fully predict catalytic activity.

The surface chemistry of SiC has not been a focus of the catalysis community, yet has been quantified in the field of electronics. The study of the oxidation of SiC by various oxygen containing molecules, e.g., $O_2$, $H_2O$, $CO_2$, and CO showed that a partial oxidation occured at the surface of SiC[73–77]. For instance, the oxidation of ∼25 nm SiC particles at room temperature by ambient $O_2$ has been shown in a study by Vaben et al.[73]. The oxide thickness was reported as effectively one atomic layer (0.16 nm), which is abnormally thin and unique to SiC due its exceedingly low element mobility[73]. Studies of high temperature (800°C) oxidation by $H_2O$, CO, and $CO_2$ also confirm the partial oxidation of the surface of SiC[74,75]. Unfortunately, the thickness of the oxide layer was not reported in these studies. Our studies of SiC under CSPR conditions for 12 hrs at an autogenous catalyst temperature of 350°C indicated that the oxidation of SiC stops at SiO and is limited to just the surface of the particles[1]. Others have reported similar results[76,77]. These results agree well with our calculations and observations that the catalyst does not oxidize to $SiO_2$ and retains catalytic activity[1]. It is noted that the thin oxide layer can be readily removed by HF etching[1,71]. Similar to GaN, the VBM of SiC would suggest that the material could evolve $O_2$, yet experiments show that this reaction is limited due to the elevated oxophilicity of SiC. Experimental surface science studies of reactivity towards carbonaceous species is quite limited over SiC, yet computational studies of others indicate strong binding of CO ($E_{ads}$ = –2.3 eV with XC functional PBE) similar to our results ($E_{ads}$ = –2.4 eV with XC functional PBE-sol)[78]. Calculations of CO and NO adsorption over SiC nanotubes also indicated appreciable surface reactivity of their surfaces[79].

### 4.2 Correlation of Computationally-Derived Mechanisms and Observed Experimental Catalyst Performance

Comparing to reliable experimental results, we first summarize our findings in concentrated solar photocatalytic reaction conditions. Reactors used were constructed from UHV conflat flange parts cleaned with a solvent sequence, baked at 600°C under flowing UHP Ar, and sealed with Cu gaskets. Doubly distilled water and SFC $CO_2$ were the only species present under reaction conditions. Many control runs were performed to verify the cleanliness of the system and that $CH_4$ and CO were produced from $CO_2$. In this reaction system, both SiC and GaN exhibited excellent photocatalytic activity towards $H_2$, CO, and $CH_4$ but dramatically different product distributions (SiC: ∼35 $\mu$mol $g^{-1}h^{-1}$ $CH_4$, ∼36 $\mu$mol $g^{-1}h^{-1}$ CO, and ∼44 $\mu$mol $g^{-1}h^{-1}$ $H_2$ and GaN: ∼3.2 $\mu$mol $g^{-1}h^{-1}$ $CH_4$ , ∼31 $\mu$mol $g^{-1}h^{-1}$ CO, and ∼3100 $\mu$mol $g^{-1}h^{-1}$ $H_2$). The contribution of lattice C to the $CH_4$ production rate was checked using water-splitting conditions at temperatures up to 350°C. $CH_4$ production rate in this case was ∼2% of that of runs performed with $CO_2$ present. SiC exhibited one of the

highest hydrocarbon production rates among verifiably organic-free systems (~35 $\mu$mol $g^{-1}h^{-1}$). GaN also exhibited one of the highest activities towards $H_2$ evolution under elevated temperature CSPR conditions (~3100 $\mu$mol $g^{-1}h^{-1}$), even comparable to highly optimized $RuO_2$/GaN:ZnO ($H_2$ evolution of ~3200 $\mu$mol $g^{-1}h^{-1}$) under UV-vis and $Rh_{2-y}Cr_yO_3$/GaN:ZnO catalysts ($H_2$ evolution of ~900 $\mu$mol $g^{-1}h^{-1}$) under visible irradiation[80–82]. At elevated reaction temperatures, $e^-/h^+$ pair recombination rate becomes a question. The temperature where this becomes appreciable is the Debye temperature. SiC exhibits much higher Debye temperature (900°C) in comparison to GaN (327°C). Despite operating slightly above the Debye temperature of GaN, a similarly improved activity to SiC was still achieved. Product selectivity for the fate of H ($CH_4$ vs. $H_2$) was 1:8 and 1:1000+ for SiC and GaN, respectively illustrating they exhibit distinctly different mechanistic features.

Considering the effect of reaction conditions in addition to the innate activity differences at ambient temperature conditions in condensed aqueous phase further underscores that the two catalysts exhibit surface chemical or electronic differences that dramatically affect their performance. Most notable are the changes in $2^{nd}$ C–O bond cleavage ability and its effect on product distribution. A preferred selectivity towards partially hydrogenated products such as $H_2CO$ (14.3 $\mu$mol $g^{-1}h^{-1}$) and $CH_3OH$ (76.4 $\mu$mol $g^{-1}h^{-1}$) has been reported over SiC under aqueous phase ambient photocatalytic reaction conditions[83]. These results were then reproduced with 100% selectivity towards $CH_3OH$ production (27.7 $\mu$mol $g^{-1}h^{-1}$) by Gondal et al. under similar conditions[84]. When reported, $CH_4$ production was noted only at trace levels[83]. Production of $H_2$ was not quantified in these studies, unfortunately. The activity of GaN at ambient temperature in condensed aqueous phase has been reported to lean heavily towards products that are not hydrogenated and $H_2$ evolution. For example, CO and $H_2$ we the only products quantified (~47 $\mu$mol $g^{-1}h^{-1}$ CO and ~570 $\mu$mol $g^{-1}h^{-1}$ $H_2$) in three different studies of GaN in $CO_2$ reduction[53,80,81]). Again, greatly diminished $CH_4$ production was encountered (~1.3 $\mu$mol $g^{-1}h^{-1}$ $CH_4$) over GaN nanowires under aqueous phase ambient temperature conditions[53].

Revisiting our results in the light of the observed activity differences of the catalysts under two distinctly different reaction conditions, we found that the effect of general surface reactivity and the nature of atomic H are likely catalyst features that dictate activity and product selectivity in the reaction. Reaction condition and the nature of the energy sources available also appear to enable different mechanistic pathways to be promoted or demoted that shift selectivity from small oxygenates to $CH_4$. Of specific interest is how elevated surface reactivity affects $H_2O$ dissociation and C–O bond cleavage and dictates hydrogenation vs. $H_2$ evolution selectivity. Calculations suggest that the stability of both surface-bound atomic H and carbonaceous intermediates correlated well with both $H_2$ evolution and $CH_4$ production selectivity over the catalysts considered. A review of the known surface chemistry of the catalysts helps to further solidify these correlations.

### 4.3 Effect of General Surface Reactivity and the Nature of Atomic H

With respect to driving $H_2O$ dissociation, catalyst surface reactivity may manipulate the surface coverage of H*, OH*, and carbonaceous intermediates and influence the general ability of the catalyst to absorb and utilize $CO_2$. Experimental performance of catalysts with lower surface reactivity, $TiO_2$ and GaN, varies considerably as a function of reaction condition. At lower temperature in condensed $H_2O$, small oxygenate production is promoted yet product distributions lean heavily towards $H_2$ production. Under CSPR conditions, these catalysts produce little to no small oxygenates and greatly improved $H_2$ evolution is encountered. On the other hand, the elevated reactivity of SiC shifts product distribution from small oxygenates at low temperature to $CH_4$ at elevated temperatures significantly. These correlations partially suggest the relative reactivity of the catalyst towards $H_2O$ and carbonaceous species that is needed to promote full $CO_2$ reduction and how their chemical potential in reaction conditions may need to be tuned. The presence of a high chemical potential of $H_2O$ in condensed phase reaction conditions may further exacerbate these effects and significantly limit the activity of catalysts with higher surface reactivity. This is most evident when comparing the performance of SiC at low and elevated temperatures, but appears to also be an issue with less reactive catalysts that still are able to effectively dissociate $H_2O$ at low temperatures. Therefore, the surface reactivity of the catalysts responsible for driving $H_2O$ dissociation may be a useful marker to partially predict overall catalyst performance and the effect of reaction conditions.

Another potential activity marker is the surface reactivity associated with driving C–O bond cleavage. Both the surface reactivity towards carbon-terminated intermediates and oxygen play a role in driving C–O cleavage and whether hydrogenation is needed beforehand. This is most evident in the degree of hydrogenation necessary to promote either $1^{st}$ or $2^{nd}$ C–O cleavage over SiC and GaN. For instance, $1^{st}$ C–O cleavage of $CO_2$ is possible with no need for hydrogenation and $2^{nd}$ C–O cleavage requires only two hydrogenations in the most favorable reaction pathway over SiC. Conversely, over GaN, significant hydrogenation is necessary before both $1^{st}$ and $2^{nd}$ C–O cleavage. Observed product distributions in different reaction conditions also support this view with small oxygenates dominant at low temperature in condensed $H_2O$ and CO, $H_2$, and $CH_4$ dominant under gas phase CSPR conditions. Promoting C–O cleavage with catalyst surface chemistry may also allow for new reaction intermediates to be present that would otherwise be absent over less reactive materials like $TiO_2$ and GaN. For instance, elevated surface reactivity of SiC towards dissociating $CO_2$ to CO* and strong binding of CO* ($E_{ads}$ = –2.4 eV) potentially presents an intermediate that is lacking over the less reactive catalysts. The ease of CO production over SiC again correlates well with both CO and $CH_4$ production. The obverse case is evident over GaN where C–O cleavage is limited and intermediates are hydrogenated to a greater degree earlier in the reaction mechanism.

The stabilization of reaction intermediates appears to be a critical aspect of photocatalysts that achieve the full reduction of

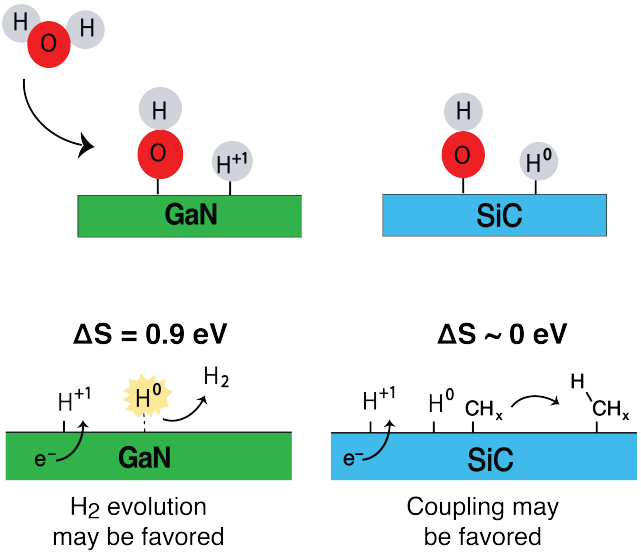


**Figure 5:** Schema to illustrate the effect of different types of surface-bound atomic H – protonic and neutral – encountered over GaN and SiC, respectively in our study. Entropy calculations for $H_2$ evolution step over GaN and a $CH_x$ fragment hydrogenation step over SiC are shown. Entropy calculation results directly correlate to experimentally observed selectivity towards $H_2$ evolution in case of GaN and $CH_4$ production in case of SiC, indicating that entropy effects may favor the production of small molecules like $H_2$ if less stable intermediates are encountered. Positive entropy change values indicate a more disordered system.

$CO_2$ to $CH_4$ and may serve as yet another activity marker. Due to the high energy reaction environment and highly endothermic reaction energetics throughout the mechanism, it is reasonable that significantly stabilized intermediates would balance and counteract the issues inherent in producing much higher energy products by limiting the kinetics for reverse reactions and promoting hydrogenation, e.g., $CH_4$ formation from $CO_2$ and $H_2O$ is endothermic by $\sim$+9.14 eV[85]. Additionally, the degree of stabilization needed may be markedly different from that appropriate for lower energy thermocatalytic reactions. Selective $CH_4$ production over SiC tracks well with more stabilized carbonaceous intermediates and atomic H, most notably in CSPR conditions where thermal energy or non-radiative vibrational excitation are available. Conversely, the relatively low surface reactivity of GaN produces less stabilized reaction intermediates including atomic H, which may enhance their unselective consumption in reverse reactions leading to the production of $H_2$ and CO. Despite both SiC and GaN exhibiting similar surface reaction energetics later in the mechanism, there is a key stopping point at CO in the reverse reaction pathway over SiC. This feature may serve to limit reoxidation of CO to $CO_2$ and enable hydrogenation to further consume this intermediate. Over GaN, intermediates may readily transform back into $H_2$ and $CO_2$ or leave the surface as $H_2$ and CO. Entropic effects that greatly favor the release of energy through the production of small molecules may also play a significant role in the reaction. If key intermediates are converted back to CO and atomic H, the high energy environment may entropically favor desorption of CO and $H_2$ over hydrogenation if the intermediates are less stable. In this case, again, more stabilized intermediates over SiC appear to limit this effect. Whereas, less stabilized intermediates over GaN correlate with significantly higher selectivity towards CO and $H_2$ production and limited $CH_4$ production.

The final activity marker suggested to control selectivity is the nature of surface-bound atomic H. The conduction band minimum edge alignments of SiC and GaN indicate both materials should present the similar H-transfer abilities, yet this does not correlate with observed selectivity between hydrogenation and $H_2$ production. Again, calculations suggest that the effective electronegativity of the photocatalyst may allow protonic H from $H_2O$ to electronically relax over solids comprised of less electronegative p-block elements than O and N. The presence of less strongly bound H of protonic nature over GaN correlated well with the fate of H ($CH_4$:$H_2$ of 1:1000+ under CSPR conditions)[1]. More stabilized neutral atomic H over SiC correlated greatly elevated selectivity towards hydrogenation for $CH_4$ production under CSPR conditions ($CH_4$:$H_2$ of 1:7).

The activity of a neutral atomic H in a photocatalytic mechanism may be unorthodox, but an understanding of the excitation of these species with energy appropriate to perform reactions has already been shown in studies of energetic electron-mediated or laser-mediated associative desorption of atomic H over metals[12,13]. In the case of a photocatalytic reaction, excited electrons may lose energy by vibrationally exciting surface-bound intermediates allowing quite significant kinetic barriers to be surmounted. This phenomenon may be promoted in CSPR conditions where a high density of excitations are present in the catalyst and has been shown to be active both over metals[12,12,28,86,87] and over a few semiconductor oxide and nitride surfaces[26,88–90]. This type of vibrational excitation is inherently different from that of thermal excitation and may produce surface electronic temperatures upwards of 1000+°C due to electronic-phonon coupling and could be responsible for surmounting some of the larger barriers we have encountered for hydrogenation events over SiC where atomic H is neutrally charged. In the ideal case, single or multiple excitations can pump the adsorbate vibrational states providing the energy needed to surmount the high H-transfer barrier for final hydrogenation of $CH_3^*$. The phenomenon may also be active over GaN, but this is not clear at this time. The stability of the atomic H after its activation via electrochemical reduction would have to be known to determine if a vibrational barrier is present in its transfer to an organic intermediate.

The transfer of neutral hydrogen, being vibration in nature, may also be directly affected by thermal inputs and detectable through kinetic isotope studies. Our previously published experimental tests of SiC at 250°C vs. 350°C have shown that elevated temperature indeed promotes hydrogenation and $CH_4$ production[1]. No such effect was observed over GaN where only protonic H is predicted to be present. Therefore, different H-transfer mechanisms may be present over the two catalysts and be connected to the ground-state oxidation state of H. Indeed, kinetic isotope effects have already been performed in our lab and have confirmed the vibrational nature of H-transfer over SiC. Whereas, the kinetic isotope effect was absent over GaN. Solid state NMR studies have further confirmed the presence of neutral H over SiC

and protonic H over GaN. These results will be presented in a follow-up publication.

Comparing our computational results with experimentally observed catalytic activity and product distributions to understand how intermediate stability may affect selectivity, we propose that the elevated surface chemical reactivity of SiC may promote enhanced $CH_4$ production with diminished $H_2$ evolution and visa versa over GaN. This suggestion is in direct agreement with all observed catalytic activity of these two materials in contamination-free systems, and appears to extend to other oxides and nitrides as well[1,53,80,82]. It is also important to note that the "appropriate" surface reactivity for photocatalytic synthesis reactions has not yet been determined, and may be dramatically different from the surface reactivity necessary to achieve activity in lower energy thermocatalytic reaction systems. Nonetheless, comparisons with observed experimental performance suggest that elevated surface reactivity may be beneficial in these reactions. It is further suggested that stabilized intermediates may facilitate coupling reaction steps and inhibit reverse reactions and entropically favored CO or $H_2$ evolution. A similar suggestion was put forth in the work of Comer et al. in the computational study of photocatalytic $NH_3$ synthesis where oxygen vacancy rich $TiO_2$ provided the most energetically favorable N–N cleavage energetics due to its elevated reactivity[19].

## 5 Conclusions

In conclusion, efforts to model the photocatalytic reduction of $CO_2$ by $H_2O$ using ground-state computational surface science techniques reveals clear connections between catalyst surface reactivity, nature of atomic H, and experimentally observed catalytic activity and selectivity. There are still significant questions surrounding the mechanisms determined and whether higher energy pathways contribute significantly or dominantly to the observed activity. However, correlations suggest that regardless of this ambiguity, accounting for general surface reactivity in catalyst selection may aid greatly in designing catalysts for $H_2$/CO or hydrocarbon production. This new understanding may also enable C2+ hydrocarbons may be accessible from $CO_2$ and $H_2O$ once appropriate surface reactivity is identified. The drawback of elevated surface reactivity is that it may limit $O_2$ evolution. Therefore, a oxygen-evolution co-catalyst is likely necessary when using carbides. The overall degree of surface reactivity that may lead to high activity and sustained selectivity towards oxygen-free products is still unclear yet the benefit of using materials more reactive than commonly used oxide and nitride photocatalysts has been established. The presence of neutral atomic H over SiC also correlates well with improved hydrogenation and elevated CH4 production. Electron-mediated reaction steps that are not photoelectrochemical in nature are well-known over metals in the surface science community and now appear to play a potentially critical role in light harvesting in photocatalytic synthesis reactions.

## Conflicts of interest

There are no conflicts to declare.

## 6 Acknowledgements

This work was supported by the National Science Foundation (NSF) under the award CHE-1465137. This work used the Extreme Science and Engineering Discovery Environment (XSEDE), which is supported by National Science Foundation grant number ACI-1548562.

## Notes and references

1 S. Poudyal and S. Laursen, *The Journal of Physical Chemistry C*, 2018, **122**, 8045–8057.
2 T. A. Westrich, K. A. Dahlberg, M. Kaviany and J. W. Schwank, *Journal of Physical Chemistry C*, 2011, **115**, 16537–16543.
3 W. Sun, C. Qian, L. He, K. K. Ghuman, A. P. Y. Wong, J. Jia, A. A. Jelle, P. G. O'Brien, L. M. Reyes, T. E. Wood, A. S. Helmy, C. A. Mims, C. V. Singh and G. A. Ozin, *Nature Communications*, 2016, **7**, year.
4 A. L. Linsebigler, G. Lu and J. T. Yates, *Chemical Reviews*, 1995, **95**, 735–758.
5 J. L. White, M. F. Baruch, J. E. Pander III, Y. Hu, I. C. Fortmeyer, J. E. Park, T. Zhang, K. Liao, J. Gu, Y. Yan, T. W. Shaw, E. Abelev and A. B. Bocarsly, *Chemical Reviews*, 2015, **115**, 12888–12935.
6 M. G. Walter, E. L. Warren, J. R. McKone, S. W. Boettcher, Q. Mi, E. A. Santori and N. S. Lewis, *Chemical Reviews*, 2010, **110**, 6446–6473.
7 X. Chen and S. S. Mao, *Chemical Reviews*, 2007, **107**, 2891–2959.
8 N. M. Dimitrijevic, B. K. Vijayan, O. G. Poluektov, T. Rajh, K. A. Gray, H. He and P. Zapol, *Journal of the American Chemical Society*, 2011, **133**, 3964–3971.
9 S. Sun, Q. An, W. Wang, L. Zhang, J. Liu and W. A. Goddard III, *Journal of Materials Chemistry A*, 2017, **5**, 201–209.
10 C. B. Layne, W. H. Lowdermilk and M. J. Weber, *Phys. Rev. B*, 1977, **16**, 10–20.
11 E. Nurlaela, T. Shinagawa, M. Qureshi, D. S. Dhawale and K. Takanabe, *ACS Catalysis*, 2016, **6**, 1713–1722.
12 D. N. Denzler, C. Frischkorn, C. Hess, M. Wolf and G. Ertl, *Physical Review Letters*, 2003, **91**, year.
13 D. N. Denzler, C. Frischkorn, M. Wolf and G. Ertl, *J. Phys. Chem. B*, 2004, **108**, 14503–14510.
14 T. Hisatomi, K. Maeda, K. Takanabe, J. Kubota and K. Domen, *Journal of Physical Chemistry C*, 2009, **113**, 21458–21466.
15 Y. Ji and Y. Luo, *ACS Catalysis*, 2016, **6**, 2018–2025.
16 Y. Ji and Y. Luo, *Journal of the American Chemical Society*, 2016, **138**, 15896–15902.
17 A. Cybula, M. Klein and A. Zaleska, *Applied Catalysis B: Environmental*, 2015, **164**, 433–442.
18 C. Yang, Y. Yu, B. van der Linden, J. C. S. Wu and G. Mul, *Journal of the American Chemical Society*, 2010, **132**, 8398–8406.
19 B. M. Comer and A. J. Medford, *ACS Sustainable Chemistry & Engineering*, 2018, **6**, 4648–4660.
20 C. Zhang, Y. Yu, M. E. Grass, C. Dejoie, W. Ding, K. Gaskell, N. Jabeen, Y. P. Hong, A. Shavorskiy, H. Bluhm, W.-X. Li, G. S.

Jackson, Z. Hussain, Z. Liu and B. W. Eichhorn, *Journal of the American Chemical Society*, 2013, **135**, 11572–11579.
21 B. M. Comer, Y.-H. Liu, M. B. Dixit, K. B. Hatzell, Y. Ye, E. J. Crumlin, M. C. Hatzell and A. J. Medford, *Journal of the American Chemical Society*, 2018, **140**, 15157–15160.
22 T. Yui, A. Kan, C. Saitoh, K. Koike, T. Ibusuki and O. Ishitani, *ACS Applied Materials & Interfaces*, 2011, **3**, 2594–2600.
23 G. Kolesov, D. Vinichenko, G. A. Tritsaris, C. M. Friend and E. Kaxiras, *The Journal of Physical Chemistry Letters*, 2015, **6**, 1624–1627.
24 W. Hou and S. B. Cronin, *Advanced Functional Materials*, 2013, **23**, 1612–1619.
25 T. E. Madey and J. T. Yates, *Journal of Vacuum Science and Technology*, 1971, **8**, 525–555.
26 U. Diebold and T. E. Madey, Desorption Induced by Electronic Transitions DIET V, Berlin, Heidelberg, 1993, pp. 284–288.
27 T. Greber, *Surface Science Reports*, 1997, **28**, 1 – 64.
28 M. Bonn, *Science*, 1999, **285**, 1042–1045.
29 G. Betz and P. Varga, *Desorption Induced by Electronic Transitions DIET IV*, Springer Berlin Heidelberg, Gloggnitz, Austria, 1990, vol. 19.
30 J. Towns, T. Cockerill, M. Dahan, I. Foster, K. Gaither, A. Grimshaw, V. Hazlewood, S. Lathrop, D. Lifka, G. D. Peterson, R. Roskies, J. R. Scott and N. Wilkins-Diehr, *Computing in Science & Engineering*, 2014, **16**, 62–74.
31 J. P. Perdew, A. Ruzsinszky, G. I. Csonka, O. A. Vydrov, G. E. Scuseria, L. A. Constantin, X. Zhou and K. Burke, *Physical Review Letters*, 2008, **100**, year.
32 G. I. Csonka, J. P. Perdew, A. Ruzsinszky, P. H. T. Philipsen, S. Lebègue, J. Paier, O. A. Vydrov and J. G. Ángyán, *Physical Review B*, 2009, **79**, year.
33 M. Bajdich, J. K. Nørskov and A. Vojvodic, *Phys. Rev. B*, 2015, **91**, 155401.
34 G. Henkelman and H. Jónsson, *The Journal of Chemical Physics*, 2000, **113**, 9978–9985.
35 G. Henkelman and H. Jónsson, *The Journal of Chemical Physics*, 1999, **111**, 7010–7022.
36 R. F. W. Bader, *Atoms in Molecules : A Quantum Theory*, Oxford University Press, New York, 1990.
37 G. Henkelman, A. Arnaldsson and H. Jónsson, *Computational Materials Science*, 2006, **36**, 354–360.
38 J. Rogal, K. Reuter and M. Scheffler, *Physical Review B*, 2007, **75**, year.
39 K. Reuter and M. Scheffler, *Physical Review B*, 2001, **65**, year.
40 Y. He and S. Laursen, *ACS Catalysis*, 2017, **7**, 3169–3180.
41 Y. He and S. Laursen, *Catalysis Science & Technology*, 2018, **8**, 5302–5314.
42 V. Bermudez and J. Long, *Surface Science*, 2000, **450**, 98 – 105.
43 V. Bermudez, *Surface Science*, 2004, **565**, 89–102.
44 X. Shen, P. B. Allen, M. S. Hybertsen and J. T. Muckerman, *The Journal of Physical Chemistry C*, 2009, **113**, 3365–3368.
45 I. A. Shkrob, N. M. Dimitrijevic, T. W. Marin, H. He and P. Zapol, *Journal of Physical Chemistry C*, 2012, **116**, 9461–9471.
46 E. E. Benson, C. P. Kubiak, A. J. Sathrum and J. M. Smieja, *Chem. Soc. Rev.*, 2009, **38**, 89–99.
47 A. J. Cowan, C. J. Barnett, S. R. Pendlebury, M. Barroso, K. Sivula, M. Grätzel, J. R. Durrant and D. R. Klug, *Journal of the American Chemical Society*, 2011, **133**, 10134–10140.
48 X. Zhang and S. Ptasinska, *Scientific Reports*, 2016, **6**, 24848.
49 P. T. Chen, C. L. Sun and M. Hayashi, *The Journal of Physical Chemistry C*, 2010, **114**, 18228–18232.
50 H. Ibach, H. Wagner and D. Bruchmann, *Solid State Communications*, 1982, **42**, 457–459.
51 F. Meyer, *Surface Science*, 1971, **27**, 107 – 116.
52 J. Du, B. Wen and R. Melnik, *Computational Materials Science*, 2014, **95**, 451–455.
53 B. AlOtaibi, S. Fan, D. Wang, J. Ye and Z. Mi, *ACS Catalysis*, 2015, **5**, 5342–5348.
54 M. Anpo, H. Yamashita, Y. Ichihashi and S. Ehara, *Journal of Electroanalytical Chemistry*, 1995, **396**, 21–26.
55 H. Yamashita, H. Nishiguchi, N. Kamada, M. Anpo, Y. Teraoka, H. Hatano, S. Ehara, K. Kikui, L. Palmisano, A. Sclafant, M. Schiavello and M. Fox, *Research on Chemical Intermediates*, 1994, **20**, 815–823.
56 K. Maeda, T. Takata, M. Hara, N. Saito, Y. Inoue, H. Kobayashi and K. Domen, *Journal of the American Chemical Society*, 2005, **127**, 8286–8287.
57 Y. F. Li, Z. P. Liu, L. Liu and W. Gao, *Journal of the American Chemical Society*, 2010, **132**, 13008–13015.
58 G. Ervin, *J American Ceramic Society*, 1958, **41**, 347–352.
59 M. Morita, T. Ohmi, E. Hasegawa, M. Kawakami and M. Ohwada, *Journal of Applied Physics*, 1990, **68**, 1272.
60 L. Trotochaud, J. K. Ranney, K. N. Williams and S. W. Boettcher, *Journal of the American Chemical Society*, 2012, **134**, 17253–17261.
61 I. C. Man, H.-Y. Su, F. Calle-Vallejo, H. A. Hansen, J. I. Martínez, N. G. Inoglu, J. Kitchin, T. F. Jaramillo, J. K. Nørskov and J. Rossmeisl, *ChemCatChem*, 2011, **3**, 1159–1165.
62 U. Roland, R. Salzer and L. Sümmchen, *Spillover and Migration of Surface Species on CatalystsProceedings of the 4th International Conference on Spillover*, Elsevier, 1997, vol. 112, pp. 339 – 348.
63 T. M. Apple, P. Gajardo and C. Dybowski, *Journal of Catalysis*, 1981, **68**, 103 – 108.
64 T. Shishido and H. Hattori, *Applied Catalysis A: General*, 1996, **146**, 157 – 164.
65 C. M. Greenlief, S. M. Gates and P. A. Holbert, *Journal of Vacuum Science & Technology A*, 1989, **7**, 1845–1849.
66 B. R. Wu and C. Cheng, *Phys. Stat. Sol. (B)*, 1994, **186**, 143–157.
67 U. Diebold, *Surface Science Reports*, 2003, **48**, 53–229.
68 Y. Yang, V. Bellitto, B. Thoms, D. Koleske, A. Wickenden and R. Henry, Silicon Carbide and Related Materials - 1999 Pts. 1 & 2, 2000, pp. 1533–1536.
69 M. A. Garcia, S. D. Wolter, T.-H. Kim, S. Choi, J. Baier, A. Brown, M. Losurdo and G. Bruno, *Applied Physics Letters*,

2006, **88**, 013506.
70 L. Smith, S. King, R. Nemanich and R. Davis, *Journal of Electronic Materials*, 1996, **25**, 805–810.
71 D. Zhuang and J. Edgar, *Materials Science and Engineering: R: Reports*, 2005, **48**, 1–46.
72 C. A. Walenta, S. L. Kollmannsberger, R. N. Pereira, M. Tschurl, M. Stutzmann and U. Heiz, *The Journal of Physical Chemistry C*, 2017, **121**, 16393–16398.
73 R. Vaben and D. Stöver, *Journal of Materials Science*, 1994, **29**, 3791–3796.
74 N. S. Jacobson, *Journal of the American Ceramic Society*, 1993, **76**, 3–28.
75 P. J. Jorgensen, M. E. Wadsworth and I. B. Cutler, *Journal of the American Ceramic Society*, 1961, **44**, 258–261.
76 X. Shen and S. T. Pantelides, *Applied Physics Letters*, 2011, **98**, 053507.
77 C. Varadachari, R. Bhowmick and K. Ghosh, *ISRN Thermodynamics*, 2012, **2012**, 1–8.
78 Y. Wang, Z. Yan, W. Liu, Q. Chen, S. Zhang and A. Hou, *Nanomaterials and Energy*, 2017, **6**, 23–28.
79 M. B. Javan, *Surface Science*, 2015, **635**, 128 – 142.
80 K. Maeda, T. Takata, M. Hara, N. Saito, Y. Inoue, H. Kobayashi and K. Domen, *Journal of the American Chemical Society*, 2005, **127**, 8286–8287.
81 K. Teramura, K. Maeda, T. Saito, T. Takata, N. Saito, Y. Inoue and K. Domen, *The Journal of Physical Chemistry B*, 2005, **109**, 21915–21921.
82 K. Maeda, K. Teramura, D. Lu, T. Takata, N. Saito, Y. Inoue and K. Domen, *Nature*, 2006, **440**, 295–295.
83 T. Inoue, A. Fujishima, S. Konishi and K. Honda, *Nature*, 1979, **277**, 637–638.
84 M. A. Gondal, M. A. Ali, M. A. Dastageer and X. Chang, *Catalysis Letters*, 2013, **143**, 108–117.
85 D. D. Wagman, J. E. Kilpatrick, W. J. Taylor, K. S. Pitzer and F. D. Rossini, *National Bureau of Standards*, 1945.
86 J. L. LaRue, T. Katayama, A. Lindenberg, A. S. Fisher, H. Öström, A. Nilsson and H. Ogasawara, *Phys. Rev. Lett.*, 2015, **115**, 036103.
87 F.-J. Kao, D. G. Busch, D. Gomes da Costa and W. Ho, *Phys. Rev. Lett.*, 1993, **70**, 4098–4101.
88 X.-Y. Zhu, M. Wolf, T. Huett and J. M. White, Desorption Induced by Electronic Transitions DIET V, Berlin, Heidelberg, 1993, pp. 63–66.
89 N. G. Petrik and G. A. Kimmel, *Physical Chemistry Chemical Physics*, 2018, **20**, 11634–11642.
90 S. L. Kollmannsberger, C. A. Walenta, A. Winnerl, S. Weiszer, R. N. Pereira, M. Tschurl, M. Stutzmann and U. Heiz, *The Journal of Physical Chemistry C*, 2017, **121**, 8473–8479.

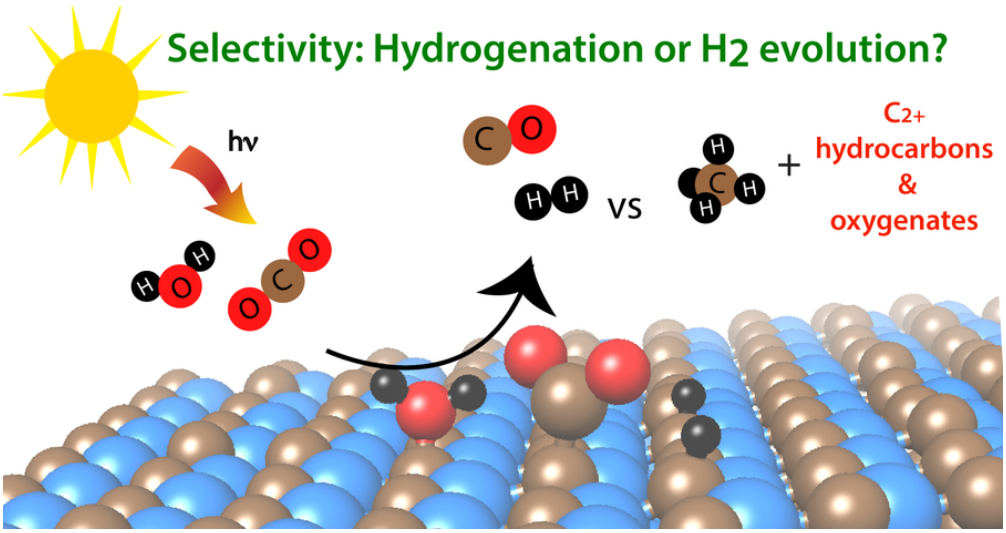


76x39mm (300 x 300 DPI)